A basic study on sound-field characteristics around an Ultrasonic Oscillator and Acoustic Streaming

Hirochika TANIGAWA [1], Hiroaki TAKEDA[2], Jiro FUNAKI[2] and Katsuya HIRATA[2*]
[1] Maizuru National College of Technology, Maizuru 625-8511, Japan

[2] Department of Mechanical Engineering, Doshisha University, Kyoto 610-0321, Japan
(khirata@mail.doshisha.ac.jp).

The sound fields produced by ultrasonic oscillators are useful for applications in various industrial aspects, such as measurements, heat/mixture enhancements, cleanings and so on. Recently, according to the development of the UVP measurement, their importance has been increasing. In this research, the authors develop a simple and high-speed computational technique to simulate the sound fields produced by oscillators with arbitrary and complicated geometies, and investigate the optimum conditions for various oscillators, numerically. Moreover, the authors simulate the acoustic streaming in a cylindrical tank, using the simulated sound field. Such numerical results are compared with experiments.

Keywords: *oscillator, sound field, ultrasonic, cylindrical container, acoustic streaming*

1 INTRODUCTION

Ultrasonic waves, strictly speaking, linear compressional waves with comparatively high frequencies, are useful for applications in various industrial aspects, such as measurements and cleaning, together with remote manipulations and non-contact transport technologies. Recently, according to the development of the ultrasonic velocity profiler (hereinafter referred to as UVP), their importance has been increasing. Moreover, ultrasonic waves can produce not only sinusoidal motions of fluid particles, but also the flow of fluid particles, even with small amplitudes. The flow is called as the acoustic streaming [1-3]. The acoustic streaming is useful as well, especially for the enhancements of heat transfers and material mixings.

Such recent increasing needs for ultrasonic waves are promoted by manufacturing cheap and robust ultrasonic oscillators such as piezoelectric actuators. The piezoelectric actuators have high flexibility in their geometries, by which we can expect widely-applicable potentials in other fields. So, we still further demand the understanding of their detailed and precise sound fields, and faster and more efficient simulation techniques.

In this research, we develop a simple and high-speed computational technique to simulate the sound field produced by ultrasonic oscillators with arbitrary and complicated geometries. Namely, we consider the sound field around an oscillator, as an ensemble of spherical waves from many point sources. Concretely speaking, we calculate the sound-pressure distributions for circular-plate, annular-plate and semi-spherical oscillators at several driving frequencies, in order to reveal the optimal frequencies and geometries. Moreover, we simulate the acoustic streaming in a cylindrical tank, using the simulated sound field. Such numerical results are compared with experiments, by which we can confirm the present numerical accuracy. Incidentally, the tested range of the non-dimensional dominant parameter $k \times a$ (for its definition, see later) is from 10-60, which is close to the value of the most common UVP probes in use.

2 COMPUTATIONAL METHOD

2.1 Velocity potential

(a) A circular-plate oscillator and other plate-type oscillators

Figure 1 shows a circular-plate oscillator, which is an oscillating-circular plate, on an infinite baffle, together with the definitions of geometrical parameters and the present coordinate system (r, φ, z). A point B denotes an arbitrary measuring point. Note that the B is on the *r-z* plane at φ = 0.

From a theoretical point of view, in order to obtain Φ, we should integrate the potential $d\Phi$ corresponding to a minute area dS on the oscillator
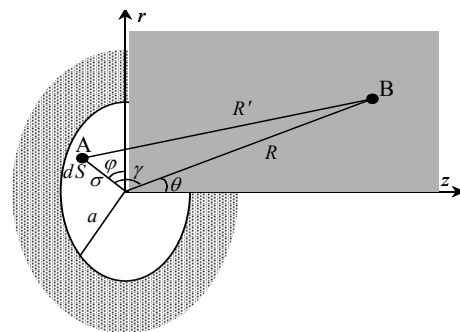

Figure 1: A circular-plate oscillator (an oscillating-circular plate) on an infinite baffle.

surface, all over the oscillator- surface areas. However, this procedure is not so easy even for simple-geometry oscillators.

Instead, we divide the oscillator into many minute sections. For example, we divide a circular-plate oscillator into $L \times M$ sections, where L and M denote the division numbers in the azimuthal and radial directions, respectively. Next, at each section, we put a point source, which is weighted by the corresponding section area. Then, we approximately regard the whole oscillator as an ensemble of $L \times M$ point sources.

As shown in Figure 1, we consider the velocity potential Φ in the complex form at the B. An arbitrary point source A with a weight of dS yields a velocity potential $d\Phi$ at the B, which are given by

$$d\Phi = \frac{\xi_0 dS}{2\pi R'} e^{j(\omega t - kR')},$$ (1)

where R' denotes the distance between the A and the B. ξ_0, ω, t and j represent velocity amplitude of the oscillator, excitation angular frequency, wave number, time and the imaginary-number unit, respectively.

Using Φ, acoustic pressure p_a is given by

$$p_a = \rho \frac{\partial \Phi}{\partial t},$$ (2)

where ρ denotes the density of fluid.

As well as the circular-plate oscillator, by the present method, we can easily calculate the sound fields produced by the oscillators with other geometries such as annuli and rectangles, if the oscillators are two-dimensional plates. For example, we merely divide an annular-plate oscillator to many minute sections in the azimuthal and radial directions, as well.

(b) A semi-spherical oscillator

We may consider three-dimensional non-plate-type oscillators, expecting the control of acoustic-wave
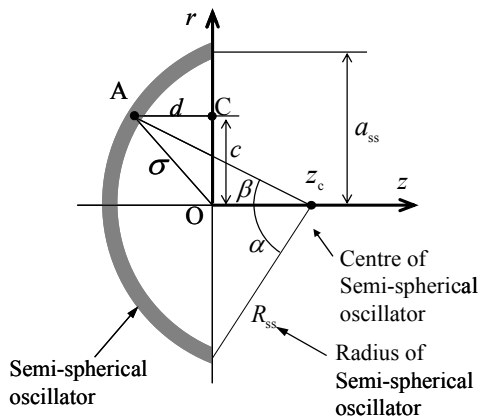

Figure 2: Sectional view of a semi-spherical oscillator.

convergence at a restricted space. Even in such cases, we can easily compute the sound field by the present method.

Figure 2 shows one of the non-plate-type oscillator, specifically speaking, the cross section on the *r-z* plane of a semi-spherical oscillator. z_c and a_{ss} represent the centre and the projected radius of the oscillator. The origin O of the coordinate system is at the centre of the oscillator's circumference. As a characteristic length scale, we consider the equivalent radius a, which defined by the radius of the circle with the same area as the oscillator surface. Then, a_{ss} is always less than a.

As well as the circular-plate oscillator, we divide the oscillator into many minute sections of $L \times M$. And, at each section, we put a point source weighted by the corresponding section area. The distance between a point source A and an arbitrary measuring point B is given by

$$R' = \sqrt{\sigma^2 + R^2 + 2R(d\cos\theta - c\sin\theta\cos\varphi)}.$$ (3)

Under the linear approximation, we should consider one non-dimensional governing parameter *k×a* on the produced sound field, together with some geometrical parameters. k denotes the acoustic wave number, which is equal to $2\pi f / c_0$, where f and c_0 represent the excitation frequency and the sound speed, respectively. Then, *k×a* is proportionate to the ratio of the oscillator size to the acoustic wave length.

2.2 Acoustic streaming

When we consider the acoustic streaming, the governing equations are the compressible-viscous-unsteady Navies-Stokes equations. In the present study, we suppose only the two-dimensional *r–z* plane, assuming the axi-symmetrical flow in a cylindrical tank. Moreover, we assume that U/c_0, u_a/c_0 and ρ_a/ρ_0 are constant values much less than unity, and that the third and the higher order terms are negligible. Then, we get the governing equations using the vorticity ζ and the stream function ψ, as follows. [2]

$$\frac{\partial \zeta}{\partial t} - \frac{1}{r}\frac{\partial \psi}{\partial z}\frac{\partial \zeta}{\partial r} + \frac{1}{r}\frac{\partial \psi}{\partial r}\frac{\partial \zeta}{\partial z} + \frac{\zeta}{r^2}\frac{\partial \psi}{\partial z}$$

$$= \nu\left(\frac{\partial^2 \zeta}{\partial r^2} + \frac{1}{r}\frac{\partial \zeta}{\partial r} + \frac{\partial^2 \zeta}{\partial z^2} - \frac{\zeta}{r^2}\right) + \left(\frac{\partial F_r}{\partial z} - \frac{\partial F_z}{\partial r}\right),$$ (4)

and

$$\frac{1}{r}\frac{\partial^2 \psi}{\partial r^2} - \frac{1}{r^2}\frac{\partial \psi}{\partial r} + \frac{1}{r}\frac{\partial^2 \psi}{\partial z^2} = -\zeta,$$ (5)

where ν denotes the kinematic viscosity of fluid. A vector $\boldsymbol{F}(F_r, F_z)$ represents the force par unit mass driven by the acoustic waves. $\boldsymbol{F}$ is given by

$$F = -\overline{(u_a \cdot \nabla)u_a} - \overline{u_a(\nabla \cdot u_a)}, \quad (6)$$

where a superscript "$^-$" represents the time-mean operation. We get the velocity vectors of fluid particle driven by acoustic waves as follows.

$$u_a = -\nabla \phi, \quad (7)$$

where the velocity potential ϕ is the real part of Φ. Time-mean flow velocity $U(U_r, U_z)$ is given by

$$U = u_0 + \frac{\overline{\rho_a u_a}}{\rho_0}, \quad (8)$$

where a subscript "0" represents the time-mean value [4].

When we consider the acoustic streaming, we need another governing parameter in addition to $k \times a$. Then, we define the acoustic Reynolds number Re_a as

$$Re_a = \frac{\xi_0 c_0}{\delta_0 \omega}, \quad (9)$$

where δ_0 denotes acoustic diffusivity. We solve the equations (4) and (5) by a finite difference method with Crank-Nicolson semi-implicit discretisation in time and 2nd-order central discretisation in space, using the SOR algebra solver.

3 EXPERIMENTAL METHOD

In the present experimental apparatus, a cylindrical tank has such dimensions as 60mm in diameter and 150mm in length. The Working fluid is glycerin aqueous solution, suspending many but small-amount-of aluminum flakes of 2-3μm inside for flow visualisation.

4 RESULTS AND DISCCUSSION

4.1 Accuracy of computed sound field

At first, we check the numerical accuracy of computed sound fields, by means of comparing them with the analytical ones obtained by Stenzel [5].
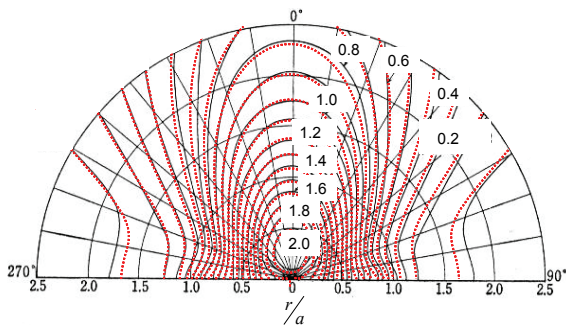

Figure 5: Contours of non-dimensional acoustic pressure amplitude $p_a'/(\rho c_0 \xi_0)$, for a circular-plate oscillator at $k \times a$ = 4. ········, Computational ; ———— , analytical (Stenzel, 1958).

Figure 5 shows contours of non-dimensional acoustic pressure amplitude $p_a'/(\rho c_0 \zeta_0)$ at $k \times a$ = 4, where $p_a' \equiv |p_a|$. Dotted and solid lines correspond to the computational and the analytical results, respectively. We can see a good agreement between them. At other $k \times a$ = 6 and 10, we also confirm good agreements.

4.2 Sound field around a circular-plate oscillator

Figure 6 shows the computed distributions of instantaneous acoustic pressure p_a (in figure (a)) and sound-pressure level $SPL \equiv 20\log_{10}(p_e/p_0)$ (in figure (b)) for a circular-plate oscillator at $k \times a$ = 55.1, where p_e denotes the effective value of acoustic pressure p_a. In Figure 6(a), we see acoustic waves
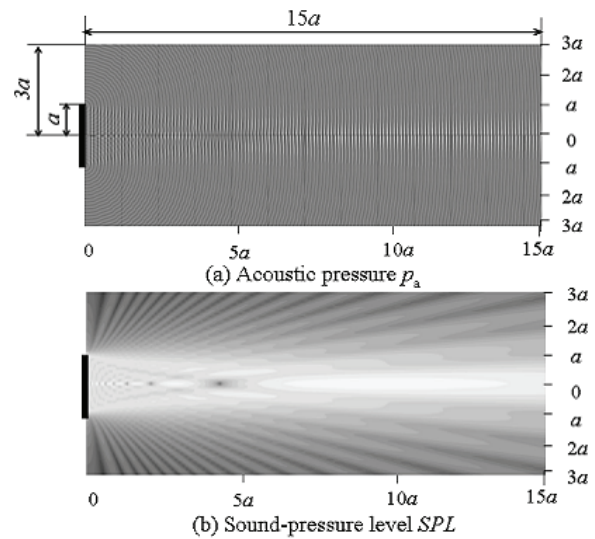

Figure 6: Distributions of p_a and SPL, for a circular-plate oscillator at $k \times a$ = 55.1 (a = 10mm, f = 1600kHz).
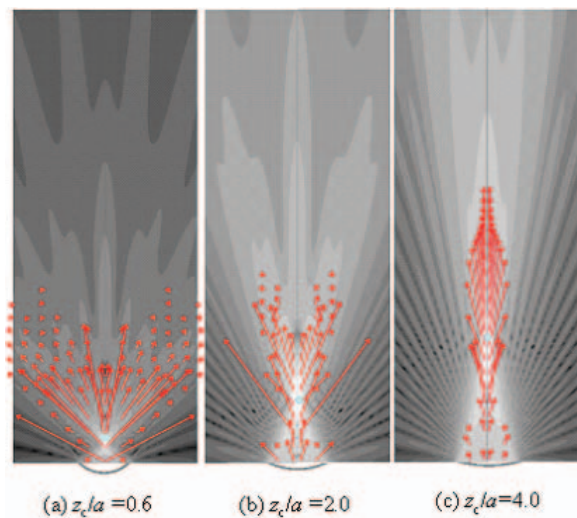

Figure 7: Distributions of sound-pressure level SPL and driving force vectors F, for around a semi-spherical oscillator at $k \times a$ = 55.1 and Re_a = 0.36 (a = 10mm, f = 1600kHz).

traveling from the oscillator, and see clear parallel stripes near the centre axis of the oscillator. the wave lengths shown by the stripes' intervals are almost equal to the plane wave theory.

Because, higher contrasts of the stripe mean larger amplitudes of p_a, we expect the strong directivity of the produced acoustic waves. In Figure 6(b), we can confirm the strong directionality.

In addition, closer to the oscillator we see, more non-uniform SPL is. Even on the centre axis, the maximum and minimum SPL s appear one after the other, with going apart from the oscillator.

4.3 Sound field around a semi-spherical oscillator

Figure 7 shows the distributions of SPL for a semi-spherical oscillator at kxa = 55.1, together with the produced driving force vectors at Re_a = 0.36. We show only the vectors with larger magnitudes than 2% of the maximum. Figures (a), (b) and (c) are at z_c/a = 0.6, 2.0 and 4.0, respectively, where z_c/a is a geometrical parameter of the oscillator. Note that the oscillator with z_c/a = ∞ is a circular-plate one. We can see that the directivity becomes weak with
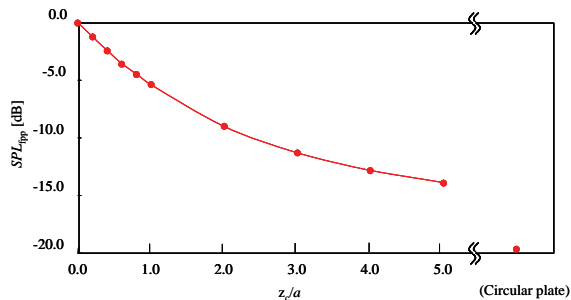

Figure 8: Sound-pressure level SPL_{fpp} at focus peak point against z_c/a, for a semi-spherical oscillator at kxa = 27.6 and Re_a = 0.36 (a = 10mm, f = 800kHz).

a) Experiment   b) Computation
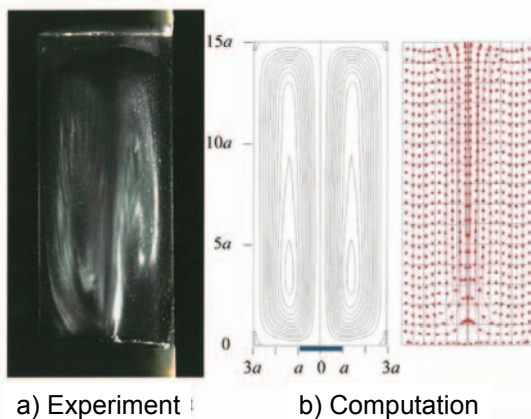
Figure 9: Comparison between experiment and computation, for a circular-plate at kxa = 27.6 and Re_a = 0.36 (a = 10mm, f = 800kHz).

decreasing z_c/a. At each z_c/a, the maximum driving force and one of the largest SPL s exist near the oscillator's focus point. Figure 8 shows the sound-pressure level SPL_{fpp} at the focus peak point plotted against z_c/a, at kxa = 27.6 and Re_a =0.36. Here, SPL_{fpp} is defined as the point where SPL attains the largest value near the oscillator's focus point. As a result, smaller z_c/a is, stronger and nearer the acoustic convergence becomes.

4.4 Computations of acoustic streaming

In order to confirm the numerical accuracy of the acoustic streaming, we investigate the mesh effect upon the maximum value of stream function ψ, at kxa = 13.8 and Re_a = 0.36. For example, a 301×61 mesh means a mesh system with 301 and 61 meshes in the azimuthal and radial directions, respectively. As the relative error of the 201×41 mesh to the 301×61 mesh is 6.4%, we use the 301×61 mesh for the other main calculations.

Figure 9 shows an acoustic streaming at kxa = 27.6 and Re_a = 0.36, both by experiment (in figure (a)) and by computation (in figure (b)). We can confirm that these results are qualitatively similar with each other.

5 CONCLUSIONS

We have developed a simple and high-speed computational technique to simulate the sound fields around complicated-geometry oscillators. The computations for a circular-plate oscillator shows a good agreement with analytical ones. Considering a semi-spherical oscillator, we have revealed the following. With decreasing z_c/a the directivity becomes weak. On the other hand, smaller z_c/a is, stronger and nearer the acoustic convergence becomes. Moreover we have simulated the acoustic streaming, and compared it with an experiment. Both are qualitatively similar with each other.

REFERENCES

[1] C. Eckert: Vortices and streams caused by sound waves, Phys. Rev., 73-1 (1948), pp.68-76.

[2] H. Mitome: Study of the generation mechanism of an acoustic jet through visualization experiments, Jpn. J. Appl. Phys. Supp., 30-1 (1991), pp.60-62.

[3] K. Matsuda, T. Kamakura and Y. Kumamoto: Theoretical study on acoustic streaming generated in a focused Gaussian beam, J. Acoustical Soc. Jpn., 50-12 (1994), pp.997-1005 (in Japanese).

[4] L. D. Rozenberg:High-intensity ultrasonic fields , Plenum Press New York (1971), pp.135-199.

[5] H. Stenzel and O. Brosze: Leitfaden zur berechnung von shhallvorgangen, Zweite Auflage, S. 77, Springer, Berlin (1958).